Neutron Absorption and Background Suppression due to Cosmic Veto

Experimental Project II : REPORT

submitted by
Anil Kumar
Research Scholar, INO, TIFR

under the supervision of
Prof. Vandana S Nanal
Dept. of Nuclear and Atomic Physics , TIFR

Contents

1 Neutron Absorption **3**
- 1.1 Introduction . . . 3
- 1.2 Gamma Ray Interaction . . . 3
  - 1.2.1 Photoelectric Effect . . . 3
  - 1.2.2 Compton Scattering . . . 4
  - 1.2.3 Pair Production . . . 4
- 1.3 Neutron Interaction with Matter . . . 4
  - 1.3.1 Slow Neutrons . . . 5
  - 1.3.2 Fast Neutrons . . . 5
- 1.4 Detector . . . 5
  - 1.4.1 $CeBr_3$ Scintillator . . . 6
  - 1.4.2 Liquid Scintillaltor . . . 6
  - 1.4.3 Photomultiplier Tube (PMT) . . . 7
- 1.5 Experimental Details . . . 7
  - 1.5.1 Sources . . . 7
  - 1.5.2 Detector Specification . . . 8
  - 1.5.3 Set Up . . . 8
  - 1.5.4 Electronics and Data Acquisition . . . 8
- 1.6 Neutron Absorption Measurements . . . 10
- 1.7 Result and Discussion . . . 13
- 1.8 Summary . . . 13

2 Background Suppression due to cosmic veto and Sensitivity **14**
- 2.1 Introduction . . . 14
- 2.2 Tifr Low background Experimental Setup (TiLES) . . . 14
- 2.3 Cosmic Veto method . . . 15
- 2.4 Sensitivity . . . 15
  - 2.4.1 ^{60}Co . . . 15
  - 2.4.2 ^{208}Tl . . . 17
- 2.5 Summary . . . 19

Bibliography **20**

Abstract

In this report, we have described two experiments: the first experiment was performed to determine the absorption coefficient of various absorbers and determine the thickness of rubber required to suppress the neutron background by the desired amount. We have also determined the thickness of rubber required for the combined absorber of rubber and lead. The second part of the report describes the background suppression due to cosmic muon in Tifr Low background Experimental Setup (TiLES) and determination of sensitivity for ^{60}Co and ^{208}Tl.

Chapter 1

Neutron Absorption

1.1 Introduction

In this experiment, we have measured the absorption of neutron through various absorbers like HDPE(Borated and non-borated), rubber and concrete etc. The aim of this experiment is to predict the thickness of rubber required to attain a given amount of background reduction. The neutrons are detected through the liquid scintillator with pulse shape discrimination method.

1.2 Gamma Ray Interaction

The gamma-ray do not have any charge hence a detector can not detect a gamma photon directly. The Gamma-ray has to transfer its energy to some other particles like electrons which can easily be detected by the detectors. There are three processes through which gamma-ray interact with matter: photoelectric effect, Compton scattering, and pair production.

1.2.1 Photoelectric Effect

In the photoelectric effect, the gamma-ray photon transfers the entire energy to atomic electrons of the detector material and disappears completely. The atomic electron has certain binding energy which is required to be transferred by photon and the remaining energy of the photon is converted into the kinetic energy of the electron.

$$K.E. = h\nu - E_b \tag{1.1}$$

where $h\nu$ is the energy of the photon and E_b is the binding energy of the electron.

The kinetic energy of the electron will be deposited in the detector and will be measured. The emitted electron leaves a vacant shell which is filled by rearrangement of other shell electrons. This rearrangement results in the emission of characteristic gamma-ray or Auger electron. The photoelectric effect is dominant for the low energy photons and high Z materials.

1.2.2 Compton Scattering

In Compton scattering, the gamma-ray transfers a partial amount of energy to the electron. The scattered gamma-ray photon has lesser energy than the incident photon. The electron gains kinetic energy as a result of Compton Scattering. This kinetic energy of the electron is deposited in the detector easily. The energy of the scattered photon is given as:

$$h\nu' = \frac{h\nu}{1 + \frac{h\nu}{m_0 c^2}(1 - \cos\theta)}, \tag{1.2}$$

where m_0 is the mass of the electron and θ is the direction of the scattered photon with respect to the incident photon. The Compton scattering is dominant at moderate gamma-ray energy and the probability of Compton scattering increases linearly with Z.

1.2.3 Pair Production

The gamma-ray photon of energy greater than 1.22 MeV results in the pair production. In pair production, a photon interacts with the high-intensity field of the nucleus and results in the production of an electron and a positron. The position has the same mass as that of the electron (511 KeV) but it is positively charged. The photon should have a minimum amount of energy which is equal to the sum of the rest mass of the particles i.e. 0.511+0.511=1.22 MeV.

The excess energy of the photon is transferred as the kinetic energy of the electron and positron. Both of them deposit their kinetic energy in the detector medium but the positron undergoes pair annihilation with some other electron and results in the two photons of energy equal to 511 KeV. If both the photon escape the detector then the total energy recorded will be the incident gamma-ray energy minus the twice of 511 KeV. This is called double escape peak. If one of the 511 KeV photons escapes the detector while the energy of the second photon is deposited in the detector. Then, the total energy deposited will be incident gamma-ray energy minus 511 KeV, this is called single escape peak. The pair production dominates for photons of high energy and medium of high Z material.

1.3 Neutron Interaction with Matter

Just like gamma-ray photons, neutrons are also chargeless particles and do not undergo Coulomb interaction with matter. Thus, a neutron can penetrate deeply into the matter and may undergo undetected in small detectors. The detection method of neutrons is based on the generation of the secondary particle when the neutron interact with the nuclei of the material medium. The neutron can undergo nuclear reaction with nuclei or get scattered through nuclei. The nuclear reaction usually generates secondary particle which interacts with matter through Coulomb interaction and can be detected easily.

The neutrons are categorized into two categories based on their energies:

1.3.1 Slow Neutrons

The neutrons with energy less than 0.5 eV are called slow neutrons. The energy transferred in the collision of neutron and nucleus of the material medium is negligible and cannot be detected by detectors. Hence, the scattering of a slow neutron with nuclei can not be used for detection purpose.

The neutron loose energy on collision with nuclei and become thermal neutron which has energy in the range 0.025 eV. The cross section for the nuclear reaction is larger for these thermal neutrons. The secondary charged particles are produced in the nuclear reaction like (n, α), (n, p) and $(n, \text{fission})$. These neutron induced reactions must have positive Q value because neutrons are having almost zero energy. The high Q-value results in the energetic secondary charged particles which are easy to detect.

1.3.2 Fast Neutrons

The neutrons with energy higher than 0.5 eV are called fast neutrons. As the energy of the neutron increases, the probability of neutron-induced nuclear reactions decreases. Thus, the fast neutrons cannot be detected through the detectors based upon the neutron induced reactions.

The fast neutron transfers a large amount of energy in the collision with the nuclei of the material medium. The nuclei either gets ejected out of lattice inelastic scattering or may result in excited states in inelastic scattering. The energetic nucleus deposits its energy in the detector medium through Coulomb interactions and thus can easily be detected by detectors. The excited nucleus in inelastic scattering usually comes to ground state by emission of the gamma-rays which deposits its energy in the detector material medium.

The larger amount of energy is transferred in case of low Z materials. The maximum energy transfer occurs when the neutron undergoes head-on collision with the hydrogen atoms, in this case, the neutron may transfer all its energy and come to rest. Thus, the neutron moderator are made of material which is rich in hydrogen-like rubber, polyethylene etc.

The collision of the fast neutron with high Z material transfers lesser amount of energy and usually result in the excited state which results in the emission of gamma-rays. Thus, the lead (Pb) is not suitable for neutron shielding become it results in the generation of the gamma-ray which increases background.

1.4 Detector

We have used $CeBr_3$ scintillator and liquid scintillator detector for the detection of gamma-ray and neutron. The basic components of the detectors are same in both cases just the detector mediums are different. The detector consists of a scintillator medium, optical coupling, and photomultiplier tube. The scintillator medium consists of a material which converts the incident particle energy into the light photons. These photons travel and reach the photomultiplier tube (PMT) through optical coupling. The photomultiplier tube has a thin layer of photocathode which converts these photons into photoelectrons through photoelectric effect and then multiplies the number of the electron which is proportional to the

incident photoelectrons. The final output of the PMT is the charge proportional to the energy of the incident particle.

1.4.1 $CeBr_3$ Scintillator

$CeBr_3$ scintillator is an inorganic scintillator. In an inorganic scintillator, the energy levels are divided into two bands valance band and conduction band. The electrons in the valence bands are loosely bond and they can absorb energy and go into the conduction band leaving a vacancy (hole) in the valence band. The conduction band electrons are free to roam around in the crystal. Whenever a conduction band electrons find a hole in the valence band, it quickly fills the vacancy and emits a photon with an energy equal to the bandgap of the material. This emission of the photon is a very inefficient process and cannot be used for scintillation purpose because the energy of these photons is higher than that of visible light. The energy gap between the valence band and conduction band is forbidden gap which means no electron can exist in those levels.

To get scintillation, an addition activator is added to the inorganic compound. This activator has energy level lying in the region of forbidden band gap. Now, the band gap structure is modified at the site where activators are present. When an energetic charged particle enters into the medium and deposits its energy, the electrons are excited to the conduction band, the holes move towards the activator sites and ionize the sites. When a conduction band electron reaches near the ionized site, it falls into the site and neutralizes it. The neutralized activator is produced in the excited state and de-excitation results into a photon of energy which lies in the visible region. Since this photon has energy lower than the bandgap of the material it cannot excite the electron in the valance band of the lattice to the conduction band. Thus, the material is transparent for this light photon.

1.4.2 Liquid Scintillaltor

The liquid scintillator consists of an organic material medium. The scintillation process occurs due to the transition across various energy levels of the organic molecules. The organic molecule possesses various electronic states and each electronic state is also accompanied by the vibrational states. The energy gap between electronic state is very large compared to the vibrational states.

When an energetic charged particle deposits energy in the detector medium, the molecules absorb the energy and go into the higher excited states. The molecules immediately come to lower excited state through non-radiative transitions. The transition from these lower excited states to the ground state results in the emission of the photon. Since the energy gap of these lower excited state from ground states is lesser compared to that of higher excited states. These emitted photons cannot re-excite the molecules and hence the material becomes transparent to the photons.

The organic molecules are rich in hydrogen atoms which can easily take energy from neutron during the collision. Once the hydrogen atoms get kinetic energy, they behave like normal energetic charged particle inside the detector medium and can be detected easily through scintillation process.

1.4.3 Photomultiplier Tube (PMT)

A photomultiplier tube or PMT receives photons and convert them into electrons which are then multiplied to get a signal pulse. The PMT is a vacuum tube consisting of photocathode, focusing electrode, dynodes, and anode.

The photocathode receives the photons and produces photoelectrons through the process of the photoelectric effect. The photon strikes the outer surface of the photocathode and the transfers its energy to the electron which diffuses toward the surface of the photocathode. The electrons with sufficient energy are able to get out of the surface of the photocathode and enter into the vacuum. High voltage is applied to the focusing electrode which creates an electric field in which electrons are accelerated towards the first dynode. The Focussing electrode decides the collection efficiency of the first dynode.

The electron striking the surface of dynode result into the emission of secondary electrons. A high voltage is applied between the successive dynodes, thus the secondary electrons emitted from the first dynode are accelerated towards the second dynode. The electrons moving towards the second dynode gains enough energy to produce more secondary electrons. The number of electrons increases as they pass through the each dynode stage. The number of secondary electrons produced by a single electron is called secondary electron ratio which depends upon the energy of electrons which in turn is dependent on the high voltage applied between two successive dynodes. Consider g be the secondary electron ratio, then after the n dynodes, a single electron will be multiplied to g^n. The electrons emitted by the n^{th} dynode are collected by the anode which gives the output to the external cable. The total charge collected depends upon the photon to electron conversion efficiency, the collection of photoelectrons, the secondary electron ratio and the number of dynode stages.

1.5 Experimental Details

In this experiment, we have measured the absorption of the neutron in various material like high-density plastic (HDPE), Rubber and Plastic etc. We have used liquid scintillator to measure neutron counts and $CeBr_3$ scintillator to measure gamma radiation generated during the absorption of the neutron in the absorber. The liquid scintillator detects both neutron and gamma radiation, we have used pulse shape discrimination technique to get the neutron counts.

1.5.1 Sources

We have used ^{241}Am/Be as neutron source which is based on the nuclear reaction of an alpha particle with the Beryllium nuclei. The alpha particle reacts with Beryllium nuclei to produce excited compound nucleus ^{13}C* which decays through a variety of modes depending on the excitation energy. In general, the dominant reaction is the decay to ^{12}C or to the 4.44 MeV excited state of ^{12}C. With ^{241}Am as an α-source, a neutron source is obtained.

We have also used various source for calibration of $CeBr_3$ like Co^{60}, Cs^{137}, Na^{22} and Thoria.

1.5.2 Detector Specification

$CeBr_3$ Scintillator

- Operating Voltage : 900 V
- Cylindrical crystal (38mm dia, 38mm long)
- 51mm diameter PMT (ETL9214) with D-20-E1-X-Neg plug-on voltage divider (breeder network) detachable
- 0.5mm Al window, External solid mu-metal shield

Liquid Scintillator

- Operating Voltage : 1400 V

1.5.3 Set Up

For this experiment, we have place liquid scintillator and source at the distance of 30 cm as shown in figure: 1.1. The $CeBr_3$ scintillator is placed beside the liquid scintillator pointing towards the source. The neutron deposits its energy through collision with the hydrogen atoms of the absorber and slows down. The slow neutron may undergo nuclear reaction with the hydrogen nucleus to produce the deuteron which has binding energy equal to 2.2 MeV. This binding energy is released in the form the gamma photon of 2.2 MeV. We have placed $CeBr_3$ detector to detect these 2.2 MeV gamma photons.

We have placed the absorber between the source and liquid scintillator at the distance of 10 cm from the source. Some neutron will be absorbed in the absorber while the remaining will reach the liquid scintillator. We are assuming that there are no scattered neutrons reaching the liquid scintillator from other directions i.e. only neutron going into straight line are reaching the detector.

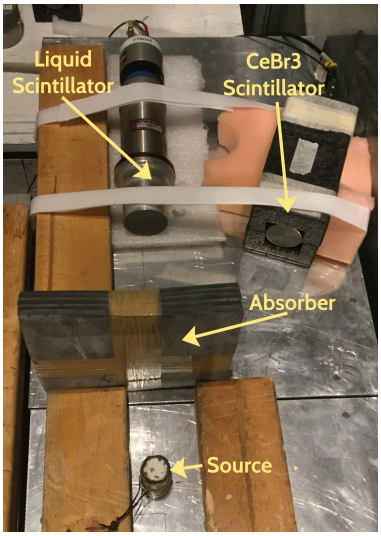

Figure 1.1: Setup

1.5.4 Electronics and Data Acquisition

For data acquisition, we have used CAEN digitizer N6751 which is a Digital Pulse Processing for Pulse Shape Discrimination firmware (DPP-PSD). The digitizer accepts signals directly from the detector and implements a digital replacement of Dual Gate QDC, Discriminator, and Gate Generator. Both the board configuration and the acquisition can be completely managed by a software interface. The CAEN DPP-PSD Control Software is a user-friendly software interface which allows the user to set the parameters for the acquisition, to configure the hardware, and to

perform the data readout. It allows also to collect the energy and PSD spectra, and to plot and to save data.

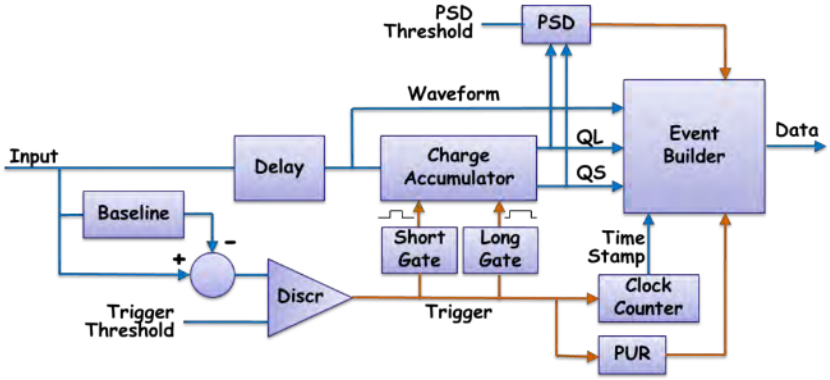

Figure 1.2: Functional Block Diagram of the DPP-PSD

The events are selected by leading edge constant fraction discriminator. The input signal baseline (pedestal) is calculated and subtracted from the energy. The charge integration can be done in two way: single gate integration for energy spectra or double gate integration for delayed and prompt pulses for pulse shape discrimination (PSD). The gate is provided by copying the signal and getting square pulse after discriminator. The other copy is delayed so to reach within the gate and charge integration is done for two different gates.

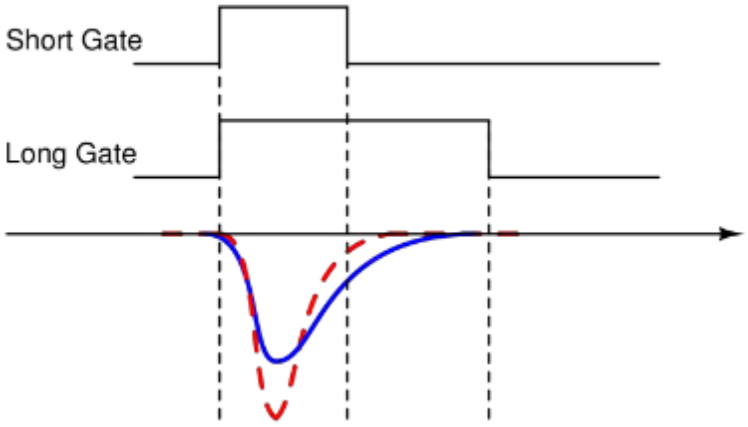

Figure 1.3: The blue pulse has a longer tail than the red one.

In liquid scintillator, the gamma ray results in prompt pulse whereas the neutron results in the delayed pulse. We select two gates of different time length called long gate and short gate. The output gives two separate charge integration for the long gate and short gate called Q_{long} and Q_{short} respectively. The ratio of charge under the tail to the total charge

Table 1.1: Parameter used in DPP-PSD firmware.

Parameter	Liquid Scintillator	$CeBr_3$
Short Gate	100 ns	70 ns
Long Gate	600 ns	300 ns
Threshold	50 LSB	50 LSB
Gate Offset	40 ns	40 ns

gives the PSD parameter which is used in the neutron-gamma discrimination:

$$PSD = \frac{Q_{long} - Q_{short}}{Q_{long}} \tag{1.3}$$

The output file is a binary file which contains a time-stamp, Q_{long} and Q_{short}. The online PSD spectrum can also be seen but we have used this binary for out data analysis.

1.6 Neutron Absorption Measurements

The purpose this experiment was to determine the absorption percent of various absorber materials. We started by measuring the neutron count without any absorber for 20 hr. Then, we placed various absorbers like HDPE1 (borated), HDPE2 (non-borated), Rubber, Plastic, concrete and Rubber+lead, the measurement were taken for 20 hr in each case.

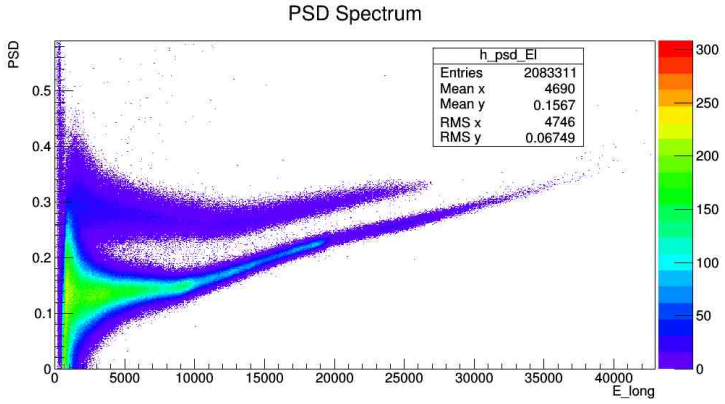

Figure 1.4: The upper region corresponds to the neutron and lower region corresponds to the gamma rays.

The 2D histogram was drawn with PSD Parameter on the y-axis and Q_{long} on the x-axis as shown in Figure 1.4. We can see two different regions corresponding to neutrons and gamma-rays. We use root software for analysis which allowed us to select the region corresponding to the neutron which was given as selecting condition to the 1D Q_{long} histogram. After the selected condition we only see the count corresponding to neutron counts, we determined the counts under the neutron region in the Figure 1.5 and registered that as neutron counts.

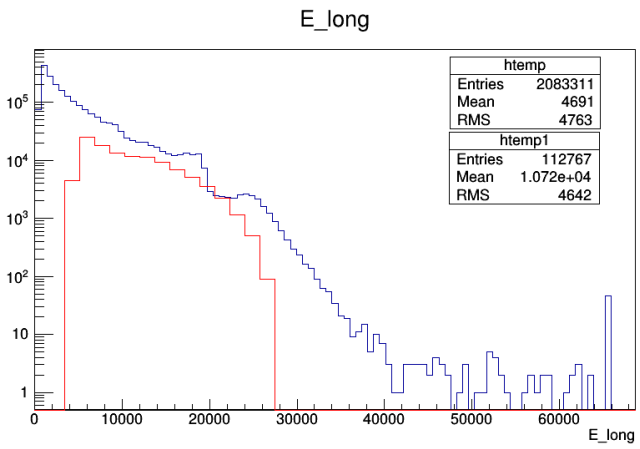

Figure 1.5: The spectrum for Q_{long} where the blue curve shows all the counts whereas the red curve shows only neutrons counts.

We have calculated the absorption percentage as follows:

$$\text{absorption} = \frac{N_{no-absorber} - N_{absorber}}{N_{no-absorber}} \times 100 \tag{1.4}$$

The 2.2 MeV and 2.6 MeV peak counts were also analyzed for various absorbers. The gamma ray spectrum used for these peaks were obtained through the $CeBr_3$ detector. The background counts were subtracted from the spectrum. While analyzing the counts, we have also removed the counts under the tails of other peaks by fitting a distribution which is Gaussian plus linear. The area under linear part corresponds to the counts from the tails of other peaks and the area under Gaussian will correspond to the true peak counts. The absorption percentage and these gamma peaks for various absorber are tabulated in Table 1.2.

Table 1.2: Absorption Measurements

Absorber	Thickness(cm)	Absorption(%)	Abs. Coef. (cm^{-1})	2.2 MeV	2.6 MeV
HDPE1(Borated)	10	70.6 +/- 0.2	0.12	868	99
HDPE2	10	71.1 +/- 0.3	0.12	5881	144
Rubber	6	47.9 +/- 0.1	0.11	*	616
Rubber	3	28.9 +/- 0.1	0.11	861	849
Plastic	5	47.4 +/- 0.1	0.13	2433	301
Plastic	10	71.9 +/- 0.3	0.13	6909	102
Concrete	10	55.8 +/- 0.2	0.08	*	691
Rubber+Pb	6+5	71.0 +/- 0.2	0.11	*	459

* Unable to do fitting due to no observable peak.

The motivation of the above experiment was to determine the thickness of rubber required to supress the neutron background by a given fraction. Consider N_0 be the number of neutron detected without any absorber and N_x be the number of neutron detected with an absorber

of thickness x. Then, N_x is related to N_0 as :

$$N_x = N_0 \exp(-\lambda x) \tag{1.5}$$

where λ is absorbtion coefficient. The rearrangement of the above equation gives:

$$\lambda = \frac{1}{x} \ln \left(\frac{1}{1 - \frac{N_0 - N_x}{N_0}} \right) \tag{1.6}$$

where $\frac{N_0 - N_x}{N_0}$ is the absorption fraction given in the table. Hence, the absorption coefficient for rubber is :

$$\lambda_{rb} = \frac{1}{6} \ln \left(\frac{1}{1 - 0.479} \right) = 0.11 \text{ cm}^{-1} \tag{1.7}$$

Assume we want to decrease the background by fraction of 10^{-4} by using rubber absorber only then we can find thickness x using Equation (1.5).

$$\frac{N_x}{N_0} = 10^{-4} \tag{1.8}$$

$$x = \frac{1}{\lambda_x} \ln \left(\frac{1}{1 - \frac{N_0 - N_x}{N_0}} \right) \tag{1.9}$$

$$x = \frac{1}{0.11} \ln(10^4) = 83.7 \approx 84 \text{ cm} \tag{1.10}$$

The combination of Rubber and Lead increases the neutron absorption and also absorbs 2.2 MeV gamma photons. Consider N_0 be the number of neutron without any absorber, N_1 be the number of neutron after passing through the rubber and N_2 be the number of neutron passing through rubber and lead both.

$$\frac{N_1}{N_0} = \exp\left(-\lambda_{rb} x_{rb}\right) \tag{1.11}$$

$$\frac{N_2}{N_1} = \exp\left(-\lambda_{Pb} x_{Pb}\right) \tag{1.12}$$

$$\frac{N_2}{N_0} = \exp -(\lambda_{rb} x_{rb} + \lambda_{Pb} x_{Pb}) \tag{1.13}$$

$$\lambda_{rb} x_{rb} + \lambda_{Pb} x_{Pb} = \ln \left(\frac{1}{1 - \frac{N_0 - N_2}{N_0}} \right) \tag{1.14}$$

$$(0.11)(6) + \lambda_{Pb}(5) = \ln \left(\frac{1}{1 - 0.71} \right) \tag{1.15}$$

$$\lambda_{Pb} = 0.12 \text{ cm}^{-1} \tag{1.16}$$

Consider that we want the backgound to be subracted by the fraction of 10^{-4}. From Equation (1.13)

$$\lambda_{rb} x_{rb} + \lambda_{Pb} x_{Pb} = \ln \left(\frac{N_0}{N_2} \right) \tag{1.17}$$

$$(0.11) x_{rb} + (0.12) x_{Pb} = \ln\left(10^4\right) \tag{1.18}$$

Suppose we want the lead to have the thickness of 5 cm then the required thickness of rubber will be :

$$(0.11)x_{rb} + (0.12)(5) = \ln(10^4) \tag{1.19}$$

$$x_{rb} = 78.3 \approx 78 \text{ cm} \tag{1.20}$$

1.7 Result and Discussion

We can see from the Table 1.2 that HDPE2 and Plastic result in the emission of significant 2.2 MeV gamma photons. The HDPE1 contains boron which undergo nuclear reaction with neutron and helps in absorption, thus, the 2.2 MeV gamma photons are lesser. The rubber is hydrogen rich, hence, it prduces some amount of 2.2 MeV gamma photons. We can see in case of rubber and lead combination the 2.2 MeV photons are absorbed by the lead. Hence, the presence of lead after rubber helps in the absorption of gamma photons generated during absorption of neutrion.

We have also calculated the thickness of rubber required to reduce the backgound by the fraction $10^{-4} = 99.99\%$ to be equal to 84 cm in case of only rubber and 78 cm in case of combination with lead of thickness 5 cm.

1.8 Summary

In this experiment, we have determined the absoprtion percentage and absorption coefficient of various materials like HDPE1, HDPE2, Concrete, rubber and rubber lead comination. We have also predicted the thickness of rubber required to reduce the neutron background by a given amount. The lead is also used in comination with rubber so as to absorb the gamma photons generated during the absorption of neutron in the rubber.

Chapter 2

Background Suppression due to cosmic veto and Sensitivity

2.1 Introduction

The double beta decay is a rare event which require very low background setup. A high efficiency, low background counting setup has been made at TIFR consisting of a special HPGe detector (≈70%) surrounded by a low activity copper+lead shield. The cosmic muons produce huge backgound to the low backgound setup because they cannot be stopped by any shield. In this report, we have removed the muon counts using cosmic muon veto. We have determined the sensitivity for ^{60}Co and ^{208}Tl after the Background Suppression due to cosmic veto.

2.2 Tifr Low background Experimental Setup (TiLES)

The TiLES consists of a low background, high efficiency HPGe detector (70% relative efficiency). The detector is a p-type HPGe with an active volume ≈ 230 cm^3 , biased to +4 kV and top Ge dead layer is 1.2 mm with a 0.9 mm carbon fiber endcap. Typical energy resolution measured is FWHM ≈ 2.2 keV at 1332.2 keV. The detector is shielded with 5 cm low activity OFHC Cu, 10 cm low activity Pb (^{210} Pb $<$ 0.3 Bq/kg), a Radon exclusion box and an active muon veto system using three plastic scintillators (P1, P2, P3). The box is an air-tight 6 mm thick Perspex box surrounding the HPGe detector as well as the Pb+Cu shield. This box volume is continuously purged with boil-off N_2 at an over-pressure of ≈ 8 mbar to reduce the Radon (^{222}Rn) contamination.

The pulses from the preamplifier of the detector are fed to a 14-bit, 100 MHz commercial CAEN-based N6724 digitizer. The digitizer produces the time stamp and the energy deposited in the detector on an event-by-event mode. The plastic scintillator signals (rise time ≈ 8 ns) are given through a fast amplifier to stretch the signal rise times in order to make it compatible with the sampling rate of the digitizer (100 MHz).

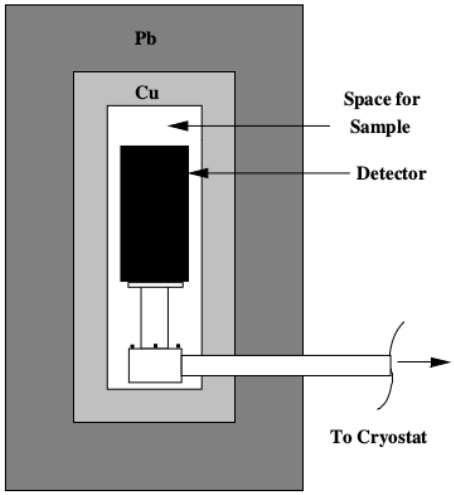

Figure 2.1: A schematic view of low background counting setup comprising the HPGe detector, $\approx$ 5 cm Cu shield, outer 10 cm low activity Pb shield and showing the space for sample.

2.3 Cosmic Veto method

We wrote an anticoincidence algorithm which finds the coincidence between the singal from HPGe detector and the muon scintillator. We rejected all those signal of HPGe detector which appear with muon signal in gate window of 2.5 μs.

2.4 Sensitivity

The measurement was taken for 3 days. The anticoincidence is done between HPGe counts and only one scintillator counts. The energy spectrum is shown in Figure 2.2 which shows few peaks at 511 KeV, 661 KeV, 1172 KeV, 1332 KeV, 2.6 MeV etc.

The analysis for 1172 KeV, 1332 KeV and 2.6 MeV peak is mentioned in this report. The counts under the peak are found by fitting the function which consist of sum of gaussian and linear functions. The area under the linear part correponds the tail of other peaks and the area under the gaussian shows the counts of the peak. The peak fitting is shown in Figure 2.3.

2.4.1 ^{60}Co

The β^- decay of ^{60}Co results in two gamma photon of energy 1173.2 KeV and 1332.5 KeV. We have measured the count of these peak in the backgound spectrum of TiLES. The decay scheme of ^{60}Co is shown in Figure 2.5 which shows the decay of ^{60}Co from 5^+ state to 2^+ or 4^+ states of ^{60}Ni.

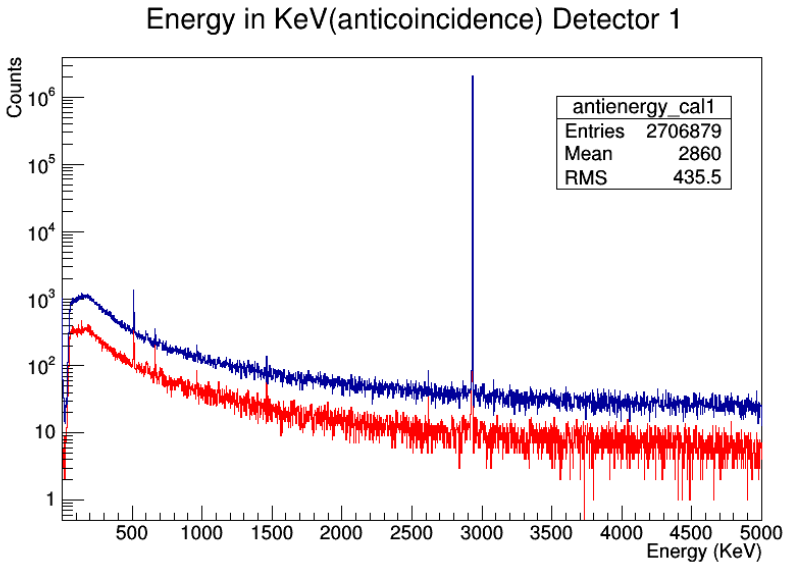

Figure 2.2: The background spectrum (blue) and supressed backgound spectrum after anti-coincidnece (red).

1173.2 KeV Peak

$$\text{Counts under the peak, } N = 82 \tag{2.1}$$

$$\text{Statistical Error in counts, } N_s = \sqrt{N} \approx 9 \tag{2.2}$$

$$\text{time, } t = 3 \text{ day} = 2.592 \times 10^5 \text{ s} \tag{2.3}$$

$$\text{Branching Ratio, } \gamma = 0.9985 \tag{2.4}$$

$$\text{Photopeak efficiency, } \epsilon = 0.021 \tag{2.5}$$

$$\text{Mass , } m = 10 \text{ g} \tag{2.6}$$

$$\text{sensitivity } = \frac{N_s}{\gamma \epsilon t m} \tag{2.7}$$

$$= \frac{9}{(0.9985)(0.021)(2.592 \times 10^5)(10)} \tag{2.8}$$

$$\approx 1.7 \times 10^{-4} = 0.17 \text{ mBq/g} \tag{2.9}$$

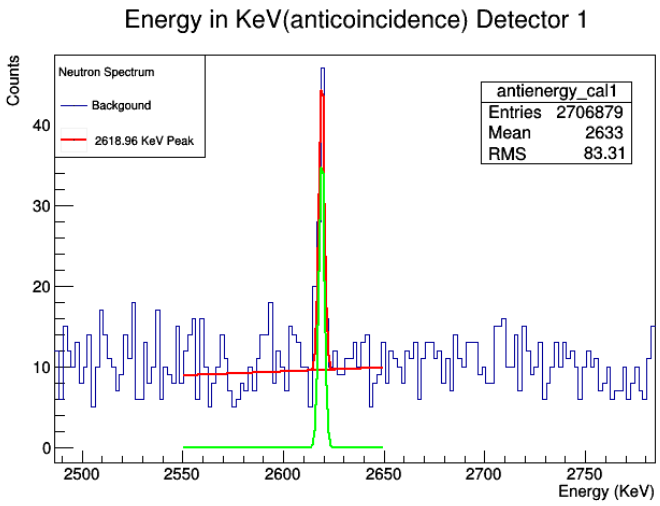

Figure 2.3: 2.6 MeV peak of ^{208}Tl

1332.5 KeV Peak

$$\text{Counts under the peak, } N = 176 \tag{2.10}$$

$$\text{Statistical Error in counts, } N_s = \sqrt{N} \approx 13 \tag{2.11}$$

$$\text{time, } t = 3 \text{ day} = 2.592 \times 10^5 \text{ s} \tag{2.12}$$

$$\text{Branching Ratio, } \gamma = 0.999826 \tag{2.13}$$

$$\text{Photopeak efficiency, } \epsilon = 0.019 \tag{2.14}$$

$$\text{Mass , } m = 10 \text{ g} \tag{2.15}$$

$$\text{sensitivity } = \frac{N_s}{\gamma \epsilon t m} \tag{2.16}$$

$$= \frac{13}{(0.999826)(0.019)(2.592 \times 10^5)(10)} \tag{2.17}$$

$$\approx 2.6 \times 10^{-4} = 0.26 \text{ mBq/g} \tag{2.18}$$

2.4.2 ^{208}Tl

The β^- decay of ^{208}Tl results in results in the 2.6 MeV photon. The decay scheme of ^{208}Tl is shown in Figure 2.6. The ^{208}Tl is a part of decay chain in Thorium series.

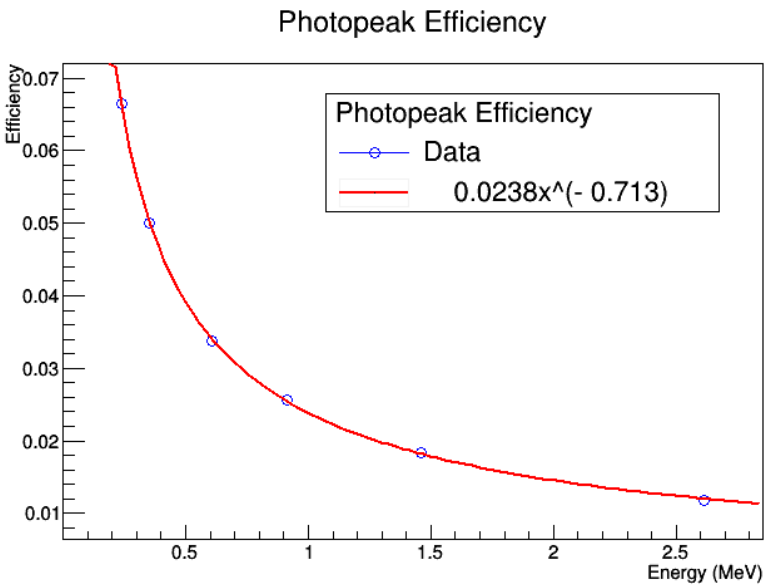

Figure 2.4: Photopeak Efficiency. Data points are generated thourgh Geant simulation considering small size source instead of background Lead shield.

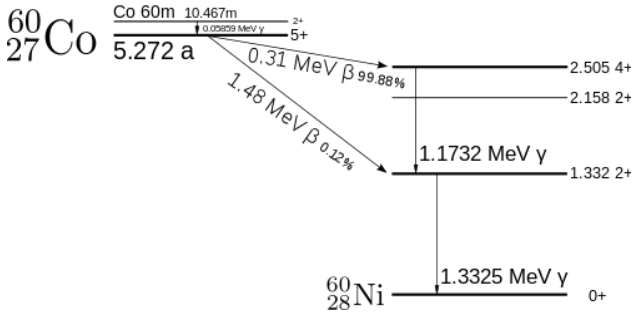

Figure 2.5: Decay Scheme of ^{60}Co

2614.5 KeV Peak

$$\text{Counts under the peak, } N = 131 \tag{2.19}$$

$$\text{Statistical Error in counts, } N_s = \sqrt{N} \approx 12 \tag{2.20}$$

$$\text{time, } t = 3 \text{ day} = 2.592 \times 10^5 \text{ s} \tag{2.21}$$

$$\text{Branching Ratio, } \gamma = 0.99754 \tag{2.22}$$

$$\text{Photopeak efficiency, } \epsilon = 0.012 \tag{2.23}$$

$$\text{Mass }, m = 10 \text{ g} \tag{2.24}$$

$$\text{sensitivity } = \frac{N_s}{\gamma \epsilon t m} \tag{2.25}$$

$$= \frac{11}{(0.99754)(0.012)(2.592 \times 10^5)(10)} \tag{2.26}$$

$$\approx 3.5 \times 10^{-4} = 0.35 \text{ mBq/g} \tag{2.27}$$

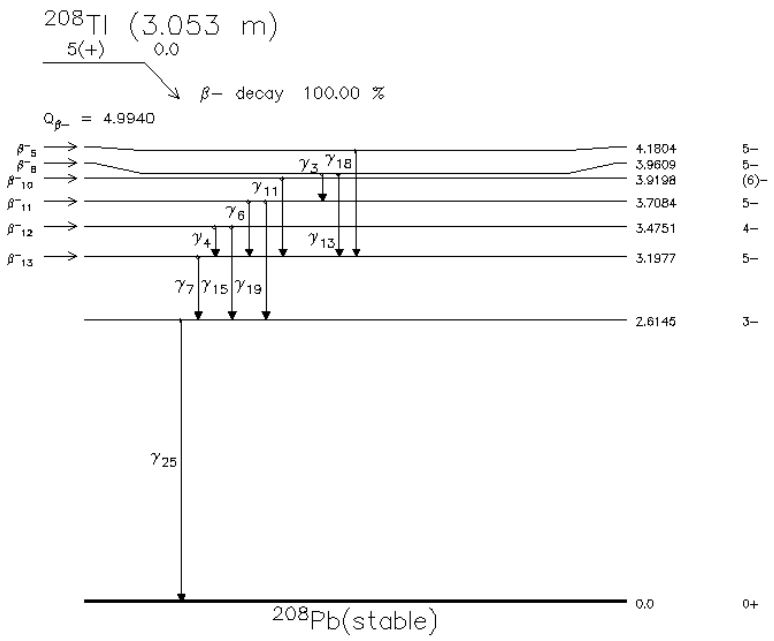

Figure 2.6: Decay Scheme of ^{208}Tl.

2.5 Summary

The relatively more muon was removed in lower energy region during anticoincidence. The sensitivity for 1173.2 KeV and 1332.5 KeV peaks of ^{60}Co was found to be 0.17 mBq/g and 0.26 mBq/g respectively. Whereas the sensitivity for 2.6 MeV peak of ^{208}Tl was found to be 0.35 mBq/g.

Bibliography

[1] *Radiation Detection adn Measurement*, Glenn F. Knoll.

[2] *Techniques for Nuclear and Particle Physics Experiments*, William R. Leo

[3] *New limit for the half-life of double beta decay of ^{94}Zr to the first excited state of ^{94}Mo*, Neha Dokania, et al. arXiv:1608.02401

[4] *Characterization and modeling of a low background HPGe detector*, Neha Dokania et.

[5] *Radiation Background Studies for Neutrinoless Double Beta Decay in ^{124}Sn*, Thesis, Neha Dokania.